Chapter 18
Geometrical Thickness Measurement of Thin Films by a Transmitted Gaussian Beam

Moisés Cywiak, Octavio Olvera-R, and Joel Cervantes-L

Abstract We describe a technique for measuring the local geometrical thickness of semi-transparent thin films by means of the diffractive properties of a transmitted Gaussian beam. In particular, we measure the semi-width of a beam transmitted through the sample with a homodyne technique especially devised for this purpose. We present analytical and experimental results with our technique.

Keywords Fourier optics and signal processing • Instrumentation, measurement, and metrology • Optical properties

18.1 Propagation of the Gaussian Beam

Measuring the thickness of a thin film, supported only by the border is a difficult task as the film vibrates continuously; thus, especial techniques have been designed for this purpose [1–13]. In this report we describe a technique based on the defocusing properties of a Gaussian beam which is accurate and has the advantage of been immune to piston-like vibration of the film.

The propagation of a Gaussian beam is well-known. A brief description follows.

In Fig. 18.1 the system is adjusted to focus the laser beam at the plane of observation with coordinates (ξ, η) in the absence of the sample, by means of a focusing lens placed on a coordinate plane (x_1, y_1) at a distance z_0 from the laser output. For simplicity the lens is considered very thin and the aperture is large enough to allow neglecting truncation of the beam. The plane of observation is adjusted at a distance z_T behind the lens to attain the best focusing conditions (minimum beam semi-width). We will refer to this plane as the best focusing plane. Once z_T has been fixed, the sample with geometrical thickness t is introduced transversally to the optical axis z in the optical path. It can be seen that,

$$z_T = z_1 + t + z_2, \tag{18.1}$$

where z_1 and z_2 are the distances depicted in Fig. 18.1 which can be chosen arbitrarily as it will be demonstrated below.

For illustrative purposes the width of the sample has been exaggerated in Fig. 18.1.

The propagation of the Gaussian beam throughout the system can be calculated by means of the Fresnel diffraction integral [14].

First, we consider a virtual sample, a slice with a refractive index equal to one and geometrical thickness t. For this condition we calculate the propagation from the laser up to the plane of observation and we plot the semi-width of the Gaussian beam as a function of distance z_T. These calculations allow characterizing all the parameters involved in the propagation of the beam.

The value of z_T in which the semi-width exhibits a minimum at the plane of observation will be referred as the best focusing distance and, as indicated, the corresponding transversal plane as the best focusing plane.

The calculations can be simplified by only characterizing the beam that emerges just after the lens. For this, we consider a circular amplitude distribution of the Gaussian just at the back surface of the lens as [15],

M. Cywiak (✉) • O. Olvera-R • J. Cervantes-L
Centro de Investigaciones en Óptica, A.C., León 37150, Guanajuato, Mexico
e-mail: moi@cio.mx

© Springer International Publishing Switzerland 2017

A. Martínez-García et al. (eds.), *Emerging Challenges for Experimental Mechanics in Energy and Environmental Applications, Proceedings of the 5th International Symposium on Experimental Mechanics and 9th Symposium on Optics in Industry (ISEM-SOI), 2015*, Conference Proceedings of the Society for Experimental Mechanics Series, DOI 10.1007/978-3-319-28513-9_18

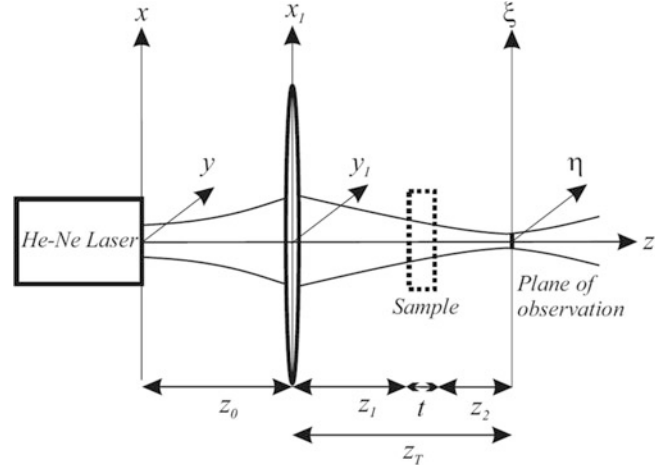

Fig. 18.1 Propagation of the Gaussian beam. z_T is set such that the plane (ξ, η) corresponds to the best focusing plane

$$\Psi_1(x_1, y_1) = A\exp\left(-\frac{x_1^2 + y_1^2}{r^2}\right)\exp\left[-i\beta\left(x_1^2 + y_1^2\right)\right]. \tag{18.2}$$

In (18.2) A is a complex constant term, r is the semi-width of the Gaussian beam and β is the corresponding coefficient of the convergent quadratic phase.

The field given by (18.2) is propagated up to the plane of observation. We obtain for the corresponding semi-width (r_A) at this plane [15],

$$r_A = \frac{\sqrt{\lambda^2 {z_T}^2 + r^4(\beta\lambda z_T - \pi)^2}}{\pi r}. \tag{18.3}$$

We emphasize that (18.3) corresponds to the case of a virtual sample with a refractive index equal to one. r_A, r, β and λ are determined experimentally as it will be described in Sect. 18.4. In this manner we propose a value for z_T which matches with our experimental conditions and it is unique.

By maintaining z_T constant, we now repeat the same calculation substituting the virtual sample by a film with a refractive index n and geometrical thickness t. The semi-width r_B in this case is given as,

$$r_B = \frac{\sqrt{\lambda^2\left(z_T - t + \frac{t}{n}\right)^2 + r^4\left(\beta\lambda\left[z_T - t + \frac{t}{n}\right] - \pi\right)^2}}{\pi r}. \tag{18.4}$$

In the next section we describe the technique for measuring the corresponding semi-widths.

18.2 Homodyne Detector

As described in [13], the homodyne detector uses a vibrating knife-edge as depicted in Fig. 18.2. The knife-edge is placed at the detection plane. For our purposes, the lens has a working distance of 1 cm allowing the placement of the sample. An attenuator (A) is included to avoid damaging the optical components due to excessive heating. A photo diode whose sensitive area is much larger than the spot size of the beam is positioned behind the knife-edge. The knife-edge is fixed to a flexure piezoelectric transducer (PZT) to vibrate in a plane transversal to the optical axis at a low frequency (f), in our case 10 Hz, with small amplitude (δ_0) of 500 nm. The PZT is also used to displace in plane the knife-edge and has high resolution of about 50 nm. A flexure type PZT is preferred as it exhibits low tilt of less than 5 µrad.

The vibrating knife-edge allows determining the semi-width of the Gaussian beam in a homodyne way as follows. First, when the knife-edge is not vibrating, due to the photodiode large sensitive area, the power collected (P) can be written as,

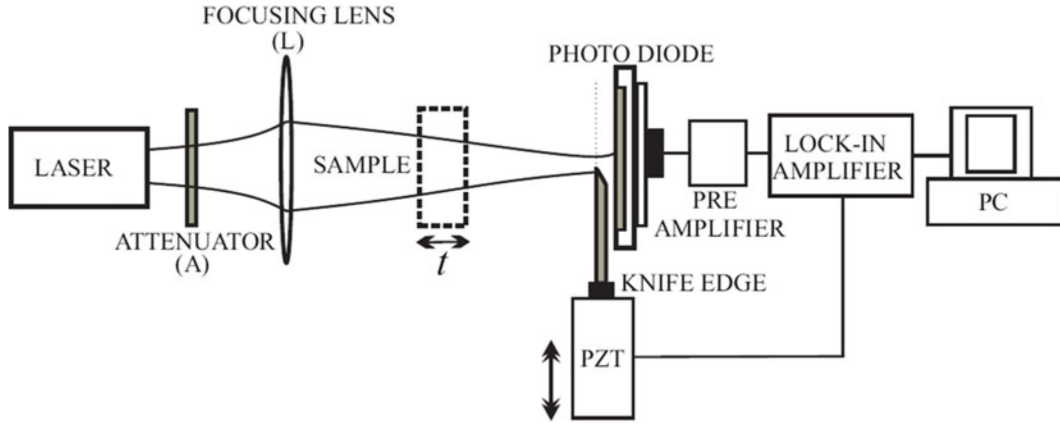

Fig. 18.2 Homodyne detector setup for measuring the semi-width and centroid of the transmitted Gaussian beam

$$P = A\int_{\alpha}^{\infty} \exp\left(-2\frac{x^2}{r_0^2}\right) dx. \tag{18.5}$$

In (18.5) A is a constant scale factor and the lower limit of the integral (α) represents the initial position of the knife-edge. r_0 is the semi-width of the beam at the plane of detection. Equation 18.5 indicates that the photodiode integrates the overall beam excluding the portion covered by the knife-edge.

Now, when the knife-edge is vibrating, the lower limit is written as,

$$\alpha = x_0 + \delta_0 \cos(2\pi f t), \tag{18.6}$$

where x_0 is a static position. By substituting (18.6) in (18.5) and by only preserving the linear term of a series expansion of the resulting equation, we obtain,

$$P_{\text{linear}}(x_0) = B\exp\left(-2\frac{{x_0}^2}{{r_0}^2}\right)\cos(2\pi f t), \tag{18.7}$$

where B is a constant. Only the first order term of the expansion has to be considered because the lock-in amplifier is tuned to the first harmonic. As a consequence, the signal detected by the lock-in results proportional to the intensity Gaussian profile evaluated at x_0 as indicated by (18.7).

To obtain the shape of the Gaussian beam with our homodyne detector it is necessary to displace the position of the knife-edge to different values of x_0. In this way, the profile and width of the Gaussian beam are obtained with high accuracy at the plane of detection.

In the next section we provide experimental results.

18.3 Experimental Section

The working conditions in our measurements were: $\beta = 4.971 \times 10^8\,\text{m}^{-2}$, $r = 2.2\,\text{mm}$, $r_A = 1.4\,\mu\text{m}$, $z_T = 1.0\,\text{cm}$, $\lambda = 0.632\,\mu\text{m}$. Refractive film index = 1.7. With these parameters r_B can be determined. With the film sample present, $r_B = 8.77\,\mu\text{m}$. Figure 18.3 depicts the experimental intensity distributions.

The acquisition time for each profile is approximately 1 min and is a consequence of the slow vibrating rate. The acquisition time can be diminished by increasing the frequency vibration of the knife-edge. For the moment being we are working in this direction.

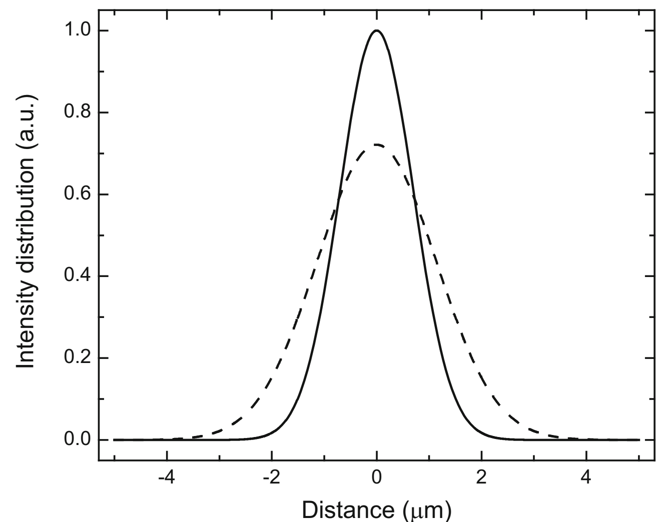

Fig. 18.3 Intensity distributions recorded with the homodyne detector normalized with respect to the virtual sample (*continuous trace*). The *dashed trace* corresponds to the measurement with the sample film

18.4 Conclusions

A technique for measuring the geometrical thickness of a semi-transparent thin film by means of the diffractive properties of a transmitted Gaussian beam has been described and tested. The technique is based on measuring the semi-width of the transmitted beam. We demonstrated that the technique is immune to piston-like vibrations of the film and as it is not interferometric, it showed to be immune to external noise. The technique was applied in determining experimentally the geometrical thickness of a commercially available stretch film.

References

1. S. Kim, J. Na, M. Kim, B. Lee, Simultaneous measurement of refractive index and thickness by combining low-coherence interferometry and confocal optics. Opt Express **16**, 5516–5526 (2008)
2. M. Ohmi, H. Nishi, Y. Konishi, Y. Yamada, M. Haruna, High-speed simultaneous measurement of refractive index and thickness of transparent plates by low-coherence interferometry and confocal optics. Meas. Sci. Technol. **15**, 1531–1535 (2004)
3. H. Maruyama, S. Inoue, T. Mitsuyama, M. Ohmi, M. Haruna, Low-coherence interferometer system for the simultaneous measurement of refractive index and thickness. Appl. Opt. **41**, 1315–1322 (2002)
4. M. Haruna, M. Ohmi, T. Mitsuyama, H. Tajiri, H. Maruyama, M. Hashimoto, Simultaneous measurement of the phase and group indices and the thickness of transparent plates by low-coherence interferometry. Opt. Lett. **23**, 966–968 (1998)
5. T. Fukano, I. Yamaguchi, Simultaneous measurement of thicknesses and refractive indices of multiple layers by a low-coherence confocal interference microscope. Opt. Lett. **21**, 1942–1944 (1996)
6. T. Fukano, I. Yamaguchi, Separation of measurement of the refractive index and the geometrical thickness by use of a wavelength-scanning interferometer with a confocal microscope. Appl. Opt. **38**, 4065–4073 (1999)
7. F. Gao, H. Muhamedsalih, X. Jiang, Surface and thickness measurement of a transparent film using wavelength scanning interferometry. Opt. Express **20**, 21450–21456 (2012)
8. P. de Groot, Measurement of transparent plates with wavelength-tuned phase-shifting interferometry. Appl. Opt. **39**, 2658–2663 (2000)
9. K. Hibino, B. Oreb, P. Fairman, Wavelength-scanning interferometry of a transparent parallel plate with refractive-index dispersion. Appl. Opt. **42**, 3888–3895 (2003)
10. G. Coppola, P. De Natale, S. De Nicola, P. Ferraro, M. Gioffre, M. Iodice, Thickness measurement of thin transparent plates with a broad-band wavelength scanning interferometer. IEEE Photon. Technol. Lett. **16**(5) (2004)
11. Y. Kumar, S. Chatterjee, Simultaneous determination of refractive index and thickness of moderately thick plane-parallel transparent glass plates using cyclic path optical configuration setup and a lateral shearing interferometer. Appl. Opt. **51**, 3533–3537 (2012)
12. Y. Kumar, S. Chatterjee, Thickness measurement of transparent glass plates using a lateral shearing cyclic path optical configuration setup and polarization phase shifting interferometry. Appl. Opt. **49**, 6552–6557 (2010)
13. O. Olvera-R, M. Cywiak, J. Cervantes-L, A. Morales, Refractive index and geometrical thickness measurement of a transparent pellicle in air by Gaussian beam defocusing. Appl. Opt. **53**, 2267–2272 (2014)
14. M. Cywiak, J. Murakowski, G. Wade, Beam blocking method for optical characterization of surfaces. Int. J. Imaging Syst. Technol. **11**, 164–169 (2000)
15. M. Cywiak, A. Morales, J. Flores, M. Servín, Fresnel-Gaussian shape invariant for optical raytracing. Opt. Express **17**, 10564–10572 (2009)